Temperature-Responsive Supramolecular Assembly and Morphology of Arborescent Copolymer Micelles with a Solvophilic Core–Solvophobic Shell Structure

ARTICLE *in* MACROMOLECULES · SEPTEMBER 2008

Impact Factor: 5.8 · DOI: 10.1021/ma801222v

5 AUTHORS, INCLUDING:

Victor C Lo
University of Sydney
11 PUBLICATIONS **138** CITATIONS
SEE PROFILE

Mario Gauthier
University of Waterloo
103 PUBLICATIONS **1,569** CITATIONS
SEE PROFILE

Abdul Munam
Sultan Qaboos University
14 PUBLICATIONS **111** CITATIONS
SEE PROFILE

Temperature-Responsive Supramolecular Assembly and Morphology of Arborescent Copolymer Micelles with a Solvophilic Core−Solvophobic Shell Structure

Seok Il Yun,*,† Gerry E. Gadd,† Victor Lo,† Mario Gauthier,‡ and Abdul Munam‡

Australian Nuclear Science and Technology Organisation, PMB 1, Menai, NSW 2234, Australia, and Department of Chemistry, Institute for Polymer Research, University of Waterloo, Waterloo, Ontario N2L 3G1, Canada

Received January 9, 2008; Revised Manuscript Received August 8, 2008

ABSTRACT: This paper describes the supramolecular assembly of arborescent (dendrigraft) copolymers in solution. The dendritic copolymers remained as unimolecular (nonassociated) micelles in toluene at temperatures above the critical self-assembly temperature (cst) but aggregated into supramolecular structures with a diameter of a few micrometers below the cst. Small-angle neutron scattering (SANS) measurements in toluene revealed that the P2VP shell of the unimolecular micelles was swollen above the cst. The supramolecular aggregates obtained below the cst had a spherical topology and a relatively uniform size according to electron microscopy analysis. The temperature-responsive self-assembly process was fully reversible. The cst varied with the copolymer concentration and shifted to higher temperatures as the length of the P2VP chains in the shell increased. The self-assembly mechanism reported provides a path to new types of "smart" supramolecular structures.

Introduction

Linear block copolymers have been investigated extensively for their ability to self-assemble into supramolecular structures that find applications in different areas including nanolithography, catalysis, molecular templating, and drug delivery.[1,2] Much emphasis in the block copolymer studies has been set on relating the characteristics of the superstructures obtained (e.g., size, morphology, uniformity) to the structure and composition of the copolymers and the conditions used for the self-assembly process.[3,4] The association behavior of dendritic macromolecules has also been examined, albeit to a more limited extent.[5−10] Dendritic polymers are a class of cascade-branched molecules including dendrimers, hyperbranched polymers, and dendrigraft (or arborescent) polymers.[10−21] In spite of the limited information available on these systems, it is clear that dendritic polymers significantly broaden the range of superstructures attainable via self-assembly. This is demonstrated, among others, by the preparation of tectodendrimers as a combination of dendritic building blocks of well-defined geometries to control the topology of the superstructures obtained.[8,9] In contrast, the self-assembly of dendrigraft polymers, the third family of dendritic polymers, is largely unexplored.

We now report, for the first time, the self-assembly of dendrigraft (arborescent) copolymers in solution, providing a new path for the creation of well-defined supramolecular structures of large dimensions. Most interestingly, the self-assembly of the arborescent copolymers investigated is temperature-responsive, offering the possibility to produce new types of "smart" supramolecular structures. Arborescent polymers incorporate linear chain segments rather than monomers as building blocks, yielding branched polymers with a very high molecular weight in a few grafting cycles (generations) while maintaining a narrow molecular weight distribution ($M_w/M_n <$ 1.1).[13−15] The generation two (G2) arborescent copolymers used in the current investigation were obtained by grafting generation one polystyrene (G1PS) substrates with poly(2-vinylpyridine) (P2VP) side chains (Scheme 1a).[14,15] Since the molecular weight of arborescent polymers grows geometrically for successive generations, the copolymers contained about 90 mol % of P2VP, even though the G1 substrate was pure polystyrene (PS). Copolymers incorporating P2VP segments have attracted much attention in the field of smart nanomaterials due to their pH responsiveness and their ability to immobilize various inorganic components for the preparation of nanoparticles.[22−24] In contrast, the temperature-responsive behavior of P2VP copolymers in toluene, while interesting, has been rarely studied. Linear and low branching functionality star PS−P2VP copolymers can self-

Scheme 1. Schematic Representation of (a) Core−Shell Morphology and (b) Temperature-Responsive Supramolecular Self-Assembly of Arborescent PS−P2VP Copolymers in Toluene

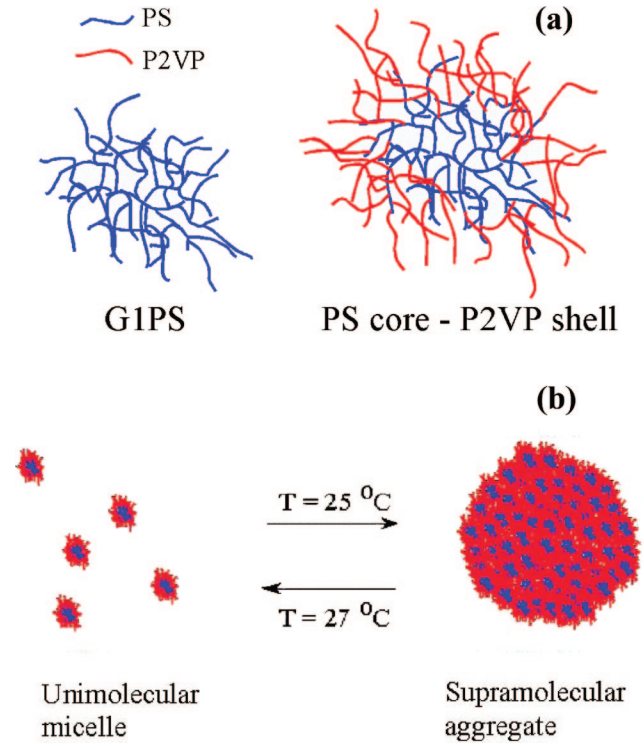

* Corresponding author. E-mail: siy@ansto.gov.au.
† Australian Nuclear Science and Technology Organisation.
‡ University of Waterloo.

10.1021/ma801222v CCC: $40.75
Published on Web 09/20/2008

Table 1. Characteristics and Thermodynamic Data for G1PS−P2VP Copolymers[a]

sample	M_n[b]/P2VP$_{branch}$ × 10^3	f_n[d]/P2VP$_{branch}$	P2VP, mol %[e]	M_n[c]	$\Delta G°$ (T = 25 °C), kJ mol^{-1}	$\Delta H°$, kJ mol^{-1}	$\Delta S°$, kJ mol^{-1}
G1PS−P2VP5K	6.2	1180	87	8.4×10^6	-18 ± 3	-190 ± 20	-0.59 ± 0.07
G1PS−P2VP30K	32.7	303	90	1.1×10^7	-43 ± 6	-560 ± 30	-1.70 ± 0.09

[a] 2VP polymerization in THF at −78 °C and grafting at room temperature (23 °C). [b] Absolute M_n of P2VP chains determined by SEC-MALLS analysis. [c] Values determined by combining the absolute M_n of the substrate with the copolymer composition from ^{1}H NMR analysis. Apparent M_w/M_n = 1.09 for G1PS−P2VP5K determined by SEC analysis using a linear polystyrene standards calibration curve. G1PS−P2VP30K was not eluted from the column. [d] Number of P2VP branches added in the last grafting reaction. [e] P2VP content determined by ^{1}H NMR analysis.

assemble into micelles in a way such that the solvophobic components of the copolymers avoid direct contact with the solvent.[25−30] Thus, the P2VP component of the copolymers, which is poorly soluble in toluene, collapses to form the core of the micelle surrounded by an expanded PS shell.[25−29] In a solvent selective for P2VP such as methanol, the core and shell components of the micelles are reversed, yielding a collapsed PS core and an expanded P2VP shell.[30]

The arborescent copolymers investigated are unimolecular micelles containing a PS core and a large number of covalently bonded P2VP chains forming a shell (Scheme 1a). Consequently, the arborescent PS−P2VP copolymers are unable to reverse their core and shell components even in a PS-selective solvent, forcing the P2VP shell to directly contact the poor solvent. This unusual micellar morphology with a solvophilic core and a solvophobic shell is interesting with respect to the core−shell structure of unimolecular micelles as well as their self-assembly. Polymer micelles are indeed typically investigated in shell-selective solvents. It should nonetheless be pointed out that the self-assembly of *charged* PS−P2VP arborescent micelles similar to the ones used in the current investigation has been observed in a mixture of methanol/HCl/water as a shell-selective solvent, in this case under the influence of electrostatic interactions.[31] In the current investigation we have discovered that in toluene arborescent copolymer micelles incorporating a PS core and a P2VP shell either remained as unimolecular micelles above the critical self-assembly temperature (cst) or formed large spherical aggregates (with a diameter of a few micrometers) below the cst (Scheme 1b). To study the influence of the P2VP chain length on the temperature-sensitive self-assembly process, P2VP side chains with a number-average molecular weight (M_n) of either 5000 (P2VP5K) or 30 000 (P2VP30K) were used. The self-assembly of arborescent copolymers in toluene was monitored using dynamic light scattering (DLS), transmission electron microscopy (TEM), and scanning electron microscopy (SEM) measurements. The unimolecular micelles of (nonaggregated) arborescent copolymers in toluene above the cst were also characterized by small-angle neutron scattering (SANS).

Experimental Section

Materials. The synthesis of the arborescent P2VP copolymers used in this study has been discussed in detail elsewhere[14,15] and is provided as Supporting Information. The M_n of the side chains was determined by size exclusion chromatography analysis of samples removed from the reactor prior to the grafting reactions. A twice-grafted arborescent polystyrene (G1PS), containing 205 side chains with M_n = 4900 (5K) and having a total $M_n = 1.1 \times 10^6$, served as grafting substrate for the preparation of both copolymers. The P2VP side chains grafted on the G1PS substrate had a M_n of either 5000 (P2VP5K) or 30 000 (P2VP30K). The characteristics of the P2VP copolymers are summarized in Table 1.

Dynamic Light Scattering (DLS). The hydrodynamic diameter (D_h) of the arborescent copolymers was determined from DLS measurements on a Malvern HPPS 3.3 instrument. The D_h of the unimolecular micelles, which have a narrow size distribution, was determined from the z-average diffusion coefficient obtained from cumulant analysis. Below the cst, the size distribution broadened due to aggregation. The D_h of the aggregates was assessed by analyzing the autocorrelation function $G(\tau)$ with a multiexponential fitting algorithm. The D_h of each fraction of the sample was calculated from the translational diffusion coefficient (D_T) derived from the analysis and the Stokes−Einstein equation, $D_T = kT/3\pi\eta D_h$, where k is the Boltzmann constant, T is the absolute temperature, and η is the solvent viscosity.

Small-Angle Neutron Scattering (SANS). The SANS experiments were carried out at the Center for Neutron Research of the National Institute of Standards and Technology, using the 30 m NIST-NG3 instruments.[32] The raw data were corrected for scattering from the empty cell, detector dark current, detector sensitivity, sample transmission, and thickness. Following these corrections, the data were placed on an absolute scale using direct beam measurement and circularly averaged to produce $I(q)$ vs q plots, where $I(q)$ is the scattered intensity, $q = \sin(\theta)4\pi/\lambda$ is the scattering vector, and θ is the scattering angle. The q range used was 0.0065−0.12 Å^{-1}, and the neutron wavelength was λ = 6 Å with a wavelength spread $\Delta\lambda/\lambda$ = 0.15.

Transmission Electron Microscopy (TEM). TEM images were recorded for samples prepared by evaporation of the copolymer solutions on holey carbon-coated grids. A JEOL 2000FXII TEM instrument operating at 100 kV with an Oxford PentaFET analytical EDS running off the Link ISIS system was used. Images were obtained using standard bright field TEM with Digital Micrograph.

Scanning Electron Microscopy (SEM). SEM images also were recorded for the samples prepared for TEM analysis. After the TEM measurements, the samples on holey carbon-coated grids were coated with 50 Å of platinum under vacuum, so as to prevent charging during the SEM experiments. This is a standard procedure known not to introduce any visible artifacts at the magnifications used here. The SEM instrument used was a JEOL JSM-6400 with an attached Noran Instruments Voyager Series IV X-ray microanalysis system. The SEM was operated at an accelerating voltage of 15 kV.

Results and Discussion

The hydrodynamic diameter D_h, measured by DLS for G1PS-P2VP5K (ϕ = 0.0014 g/mL) in methanol and toluene, as a function of temperature, is provided in Figure 1a. The D_h of the copolymer in methanol, a good solvent for the P2VP shell, remained almost independent of temperature, and no aggregation was observed, in agreement with previous results.[33] The copolymer did not disperse well in toluene at temperatures below 26 °C, as expected for this copolymer containing 87 mol % of insoluble P2VP branches in the shell. Interestingly, above 26 °C, the solution became transparent and the copolymer was molecularly dissolved with a $D_h = 57 \pm 3$ nm. The size of the molecularly dissolved G1PS−P2VP5K copolymer in toluene at these higher temperatures was about 10% lower than in methanol, indicating shrinkage of the P2VP shell in toluene due to the poorer solvent quality. By decreasing the temperature from 27 to 25 °C, the D_h increased abruptly to a few micrometers, as shown in Figure 1a. In contrast to the nonassociated copolymers having a uniform size distribution (error bars smaller than the data point markers in Figure 1), these large aggregates had a somewhat broad size distribution (large error bars), but nonetheless a well-defined spherical topology (vide infra). The DLS measurements confirmed that the supramolecular structures persisted at the lower temperatures, albeit some

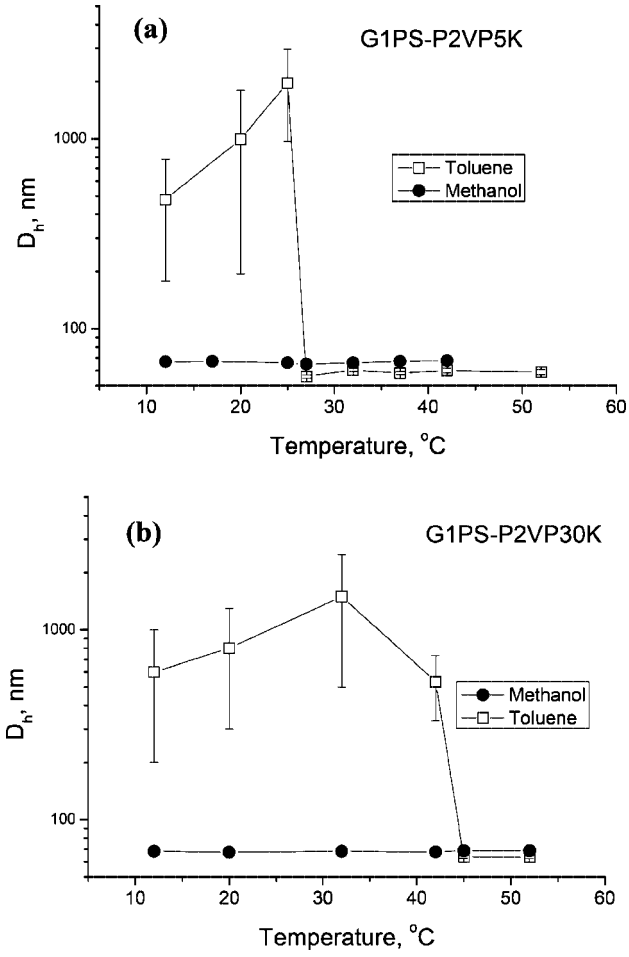

Figure 1. Hydrodynamic diameter of (a) G1PS−P2VP5K and (b) G1PS−P2VP30K obtained from DLS in methanol and toluene as a function of temperature. The concentration of all solutions was ϕ = 0.0014 g/mL.

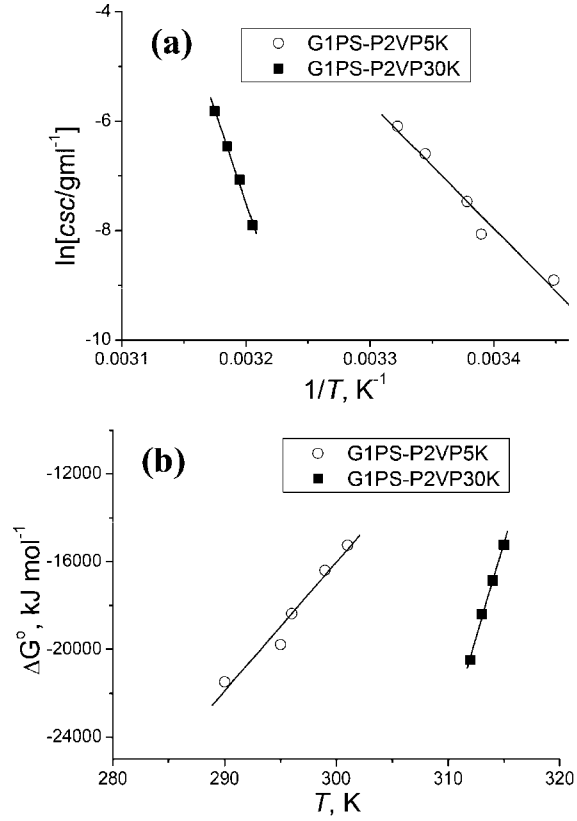

Figure 2. Variation in (a) the critical self-assembly concentration (csc) and (b) the Gibbs free energy ($\Delta G°$) with temperature for G1PS−P2VP5K and G1PS−P2VP30K in toluene.

of the larger aggregates precipitated as the temperature was decreased below 20 °C. Since the precipitation was time-dependent, the D_h values measured by DLS below 20 °C likely do not reflect the actual size of the precipitated aggregates. We did not intend to study the kinetics of aggregation in the current investigation. The aggregation transition was thermoreversible, the size decreasing back to that of the isolated molecules at 27 °C, as illustrated in Figure 1a and Scheme 1b. The reversible size transition between 25 and 27 °C occurred within the 1−3 min cooling or heating cycle of the DLS instrument.

The D_h values measured by DLS for G1PS−P2VP30K (ϕ = 0.0014 g/mL) with longer P2VP chains in methanol and in toluene as a function of temperature are also provided in Figure 1b. Similar thermoreversible self-assembly was observed, but the critical self-assembly temperature (cst) was shifted to a higher temperature (41 °C) in that case. This shows that the critical temperature for the thermoresponsiveness is tunable by varying the length of the P2VP segments within the shell. For comparison, the copolymer grafted with shorter (P2VP5K) side chains at the same concentration displayed no aggregation whatsoever at 27 °C. Clearly, the aggregation becomes more favorable as the size of the insoluble branches increases. The micellization of amphiphilic PS−P2VP copolymers in toluene, driven by solvophobic interactions of the P2VP chains, was previously reported to depend strongly on temperature as well as molecular architecture.[25−29] In analogy to arborescent PS−P2VP, star-shaped copolymers have been reported to remain molecularly dissolved without association in toluene at higher temperatures, but to aggregate into large micelles at low temperatures (<40 °C). Interestingly, linear PS−P2VP block copolymers aggregated even at higher temperatures, indicating that the micellization of linear block copolymers is more favorable than for star copolymers.[27]

Similarly to the critical micelle concentration (cmc) of the closed association model for micellization, the critical self-assembly concentration (csc) of arborescent PS−P2VP copolymers at 25 °C was determined by DLS. The standard Gibbs free energy for self-assembly at 25 °C was calculated from the equation $\Delta G° = RT \ln(\text{csc})$. From the temperature dependence of the csc (Figure 2a) the standard enthalpy of self-assembly, $\Delta H°$, was obtained using the Gibbs−Helmholtz equation, $\Delta H° = R[\mathrm{d} \ln(\text{csc})/\mathrm{d}T^{-1}]$. The standard entropy for self-assembly, $\Delta S°$, was calculated from the slope of a linear plot of $\Delta G°$ vs T (Figure 2b), in accordance with the equation $\Delta G° = \Delta H° - T\Delta S°$. The thermodynamic properties thus obtained for the arborescent copolymers are summarized in Table 1. The negative $\Delta G°$ values indicate that the self-assembly of arborescent PS−P2VP copolymers in toluene is thermodynamically favorable due to the solvophobic interactions of the P2VP shell. Because of the weak scattering intensity at very low concentrations, the csc = 2.4×10^{-8} g/mL was estimated for G1PS−P2VP30K containing longer P2VP branches by extrapolating the plot of ln(csc) vs T^{-1} to T = 25 °C. The $\Delta G°$ value at 25 °C was more negative for the arborescent copolymers with longer (P2VP30K) branches, confirming the more favorable aggregation for copolymers with longer insoluble branches. Similarly, $\Delta G°$ was reported to become more negative for star PS−P2VP copolymers in toluene as the length of the insoluble P2VP arms increased.[18,19] The large negative values of $\Delta H°$ indicate that the self-assembly of both arborescent PS−P2VP copolymers is an enthalpically favorable process. The standard entropy of aggregation $\Delta S°$ was negative, showing that the

entropic contribution is unfavorable. Interestingly, $\Delta S°$ was much more negative for arborescent copolymers with longer (P2VP30K) branches than for those with 5K branches. This demonstrates that the entropy loss of arborescent copolymers is dependent on the length of the insoluble block. Since the entropy loss was more significant for arborescent PS−P2VP30K than for PS−P2VP5K, the large negative $\Delta H°$ for PS−P2VP30K is therefore responsible for the more favorable aggregation (more negative $\Delta G°$) for PS−P2VP30K. It is also interesting to note that the size of the superstructures formed by linear- or star-shaped block copolymers (50−60 nm)[27,28] was much smaller than for the aggregates of arborescent PS−P2VP copolymers (1−3 μm). This is obviously due to the characteristics of arborescent polymers, with very high branching functionalities and M_n even for relatively low generations such as the G2 samples investigated.

The morphology of the arborescent unimolecular micelles in a core-selective solvent is of particular interest because of the possibility to form a swollen core and a partly collapsed shell (solvophilic core−solvophobic shell) even above the cst. Unimolecular micelles with collapsed P2VP arms and swollen PS arms were indeed pictured even for heteroarm star copolymers in toluene above the critical micelle temperature.[27] Monte Carlo simulation studies on the conformation of dendrimer micelles with a solvophilic core and a solvophobic shell likewise predicted that the solvophobic monomer units in the shell would collapse into the core while the solvophilic inner segments rearrange and form a corona.[34,35] The morphology of the arborescent copolymers in toluene-*d* above the cst was investigated by SANS. The internal segment density of the arborescent micelles was first assessed by fitting the SANS data with a core−shell model using two different constant density values in the core and shell regions of the sphere. This model has been successfully used to characterize the internal structure of many micellar systems because it gives the effective average density values of each region. The small-angle neutron scattering intensity from a suspension of monodipersed spheres can be written as[36]

$$I(q) = NF(q)^2 \tag{1}$$

$$F(q) = \left[\int (\rho(r) - \rho_{\text{solvent}}) \frac{\sin qr}{qr} 4\pi r^2 \, \mathrm{d}r \right] \tag{2}$$

where N is the number density of particles, $\rho(r)$ is the scattering length density (SLD) in the sphere, and ρ_{solvent} is the SLD of the solvent. For a sphere with radius R_2 that has an inner core with a radius R_1, the following analogous equation is obtained.

$$I(q) = N\left[\int_0^{R_1} (\rho_{\text{core}} - \rho_{\text{solvent}}) \frac{\sin qr}{qr} 4\pi r^2 \, \mathrm{d}r + \int_{R_1}^{R_2} (\rho_{\text{shell}} - \rho_{\text{solvent}}) \frac{\sin qr}{qr} 4\pi r^2 \right]^2 \tag{3}$$

In order to handle size polydispersity, eq 1 was averaged over the particle size distribution using a Schultz distribution.[36] The SANS data obtained for the arborescent copolymers and the best fits using the core−shell model are compared in Figure 3a. The fitting parameters ρ_{core} and ρ_{shell} are related to the radial density profiles by the equations

$$\rho_{\text{core}} = C_{\text{PS}}\rho_{\text{PS}} + (1 - C_{\text{PS}})\rho_{\text{solvent}}$$
$$\rho_{\text{shell}} = C_{\text{P2VP}}\rho_{\text{P2VP}} + (1 - C_{\text{P2VP}})\rho_{\text{solvent}} \tag{4}$$

where C is the volume fraction of (dry) polymer in the core and shell. The radial polymer volume fraction profiles for the individual molecules, as obtained from the core−shell model fits, are displayed in Figure 3b. For comparison, the polymer

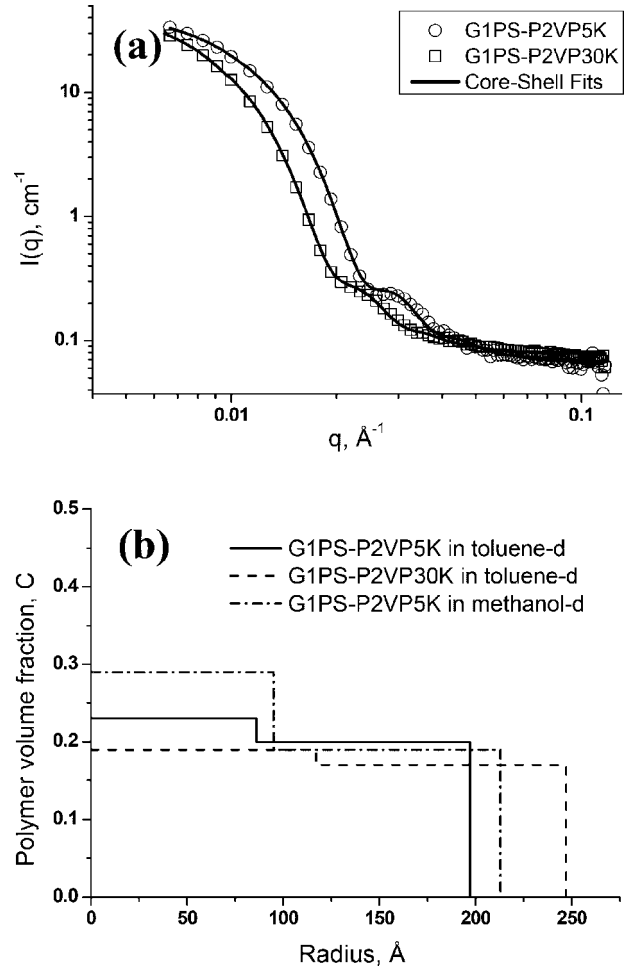

Figure 3. (a) SANS data for G1PS−P2VP5K (ϕ = 0.0034 g/mL) and G1PS−P2VP30K (ϕ = 0.0034 g/mL) in toluene-*d* at 75 °C and best fits using the core−shell model. The fit of the data includes about 10% polydispersity in size for the polymers and instrumental smearing effect. (b) Polymer fraction profiles for the copolymers in toluene-*d* derived from the core−shell model fits.

volume fraction profile for G1PS−P2VP5K in methanol-*d*, which is a selective solvent for the P2VP shell, is also displayed in Figure 3b. The PS core of G1PS−P2VP5K appears to be more swollen (smaller C value) in toluene-*d* than in methanol-*d*, as anticipated. The P2VP shell in toluene-*d* is slightly less swollen than in methanol-*d* but still fairly expanded, in spite of the poor solvent quality of toluene for P2VP. The G1PS−P2VP30K sample, with the longer P2VP chains in the shell, exhibited even more swelling in toluene-*d* than G1PS−P2VP5K, possibly due to the more flexible character of the longer P2VP chains. The swollen core and shell morphology observed indicates that the P2VP chains within the shell, when exposed to a poor solvent, did not collapse into the core region, in contrast to Monte Carlo simulation results for dendrimer micelles with a solvophobic shell and a solvophilic core.[33,34] This difference may be due to toluene-*d* above the cst being simply not poor enough to induce the collapse of the P2VP shell chains. As the solvent quality decreased (below the cst), the arborescent micelles did not remain in their unimolecular state but rather aggregated, in contrast to dendrimers burying their solvophobic end groups into the core to avoid unfavorable contacts with the solvent and lower their overall free energy. Since the building blocks of arborescent polymers are bulky linear segments ($DP_n \approx 50$ or 300 monomer units), the collapse of the P2VP chains into the highly branched PS core would be much more energy-demanding than for the rearrangement of chain segments in low

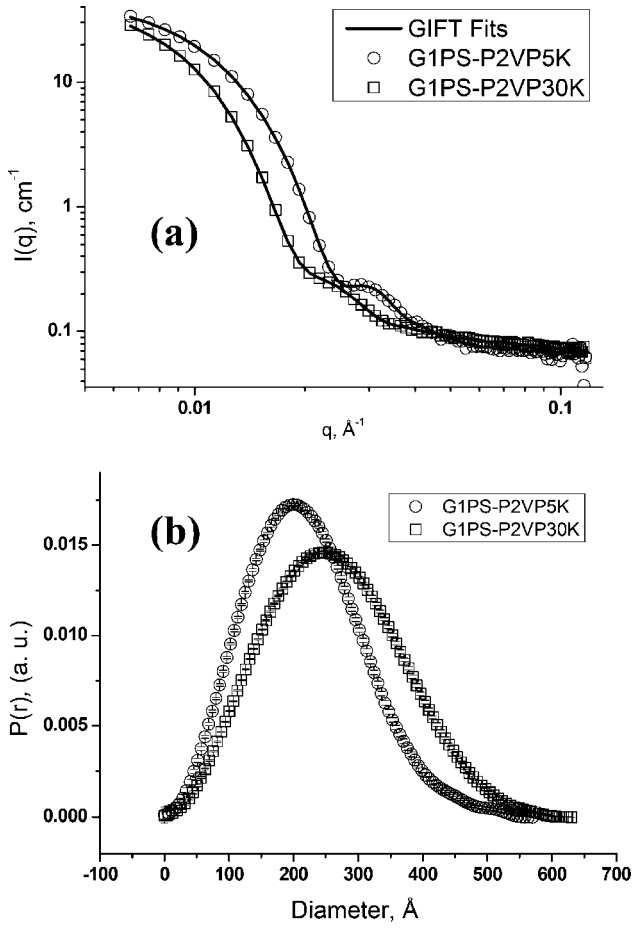

Figure 4. (a) Experimental SANS data for G1PS−P2VP5K ($\phi = 0.0034$ g/mL) and G1PS−P2VP30K ($\phi = 0.0034$ g/mL) in toluene-*d* at 75 °C and fits by the IFT method using the GIFT program. (b) Corresponding PDDF.

branching functionality star polymers or for the chain ends of dendrimers. The question of solvent quality of course comes into play (worse solvent = larger driving force for conformation changes), but since arborescent polymers have a limited ability to rearrange they can only precipitate out of solution.

The simulations also predicted that end-group segregation within the core of dendrimer micelles would result in elongation or a dumbbell-like conformation for dendrimer micelles.[34,35] The good fit of the core−shell sphere model to the SANS data is consistent with arborescent micelles adopting a spherical rather than an elongated shape even under poor shell solvency conditions (considering that toluene is a poor solvent over the whole temperature range investigated). Alternatively to the model fit according to eqs 1 and 2, indirect Fourier transformation can be performed on the SANS data to determine the overall shape of scattering objects. The scattering intensity $I(q)$ is related to the real space pair distance distribution function (PDDF) by the following Fourier transformation, which enables the determination of the overall shape and size of scattering objects.[37]

$$I(q) = 4\pi \int_0^\infty p(r)\frac{\sin(qr)}{qr}\,\mathrm{d}r \qquad (5)$$

The PDDF under good solvency conditions for both the core and the shell of arborescent copolymers were previously determined by the SANS contrast matching method and confirmed that arborescent polymers are spherical macromolecules with a core−shell morphology.[38] The PDDF obtained for both G1PS−P2VP5K and G1PS−P2VP30K, provided in Figure 4, does not have two maxima or a skewed distribution,

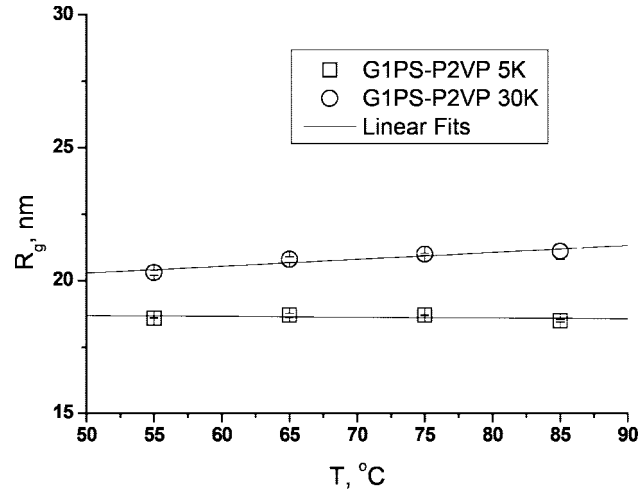

Figure 5. Influence of temperature on R_g for G1PS−P2VP5K and G1PS−P2VP30K in toluene-*d* extrapolated to $\phi = 0$.

typical for dumbbell-like and elongated shapes, respectively. The bell-shaped PDDF obtained for both copolymers is typical for a well-defined spherical topology, confirming that poor shell solvency conditions did not alter the shape of arborescent micelles.[39]

The radius of gyration (R_g) was determined from Guinier plots of the SANS data at different concentrations (0.001 g/mL < ϕ < 0.007 g/mL) according to the equation $I(q) = I(0)\exp(-R_g^2q^2/3)$ (the Guinier plots are supplied as Supporting Information). The R_g obtained at different concentrations were extrapolated to $\phi = 0$ (see Supporting Information). The extrapolated R_g ($\phi = 0$) values in toluene-*d* are provided as a function of temperature (55 °C < T < 85 °C) in Figure 5. The radius of gyration of the molecules in toluene-*d* is essentially constant for G1PS−P2VP5K but decreases slightly (<5%) for G1PS−P2VP30K as the temperature decreases. The ratio P = radius of gyration (R_g)/hydrodynamic radius (R_h) is a sensitive fingerprint of the internal density profile of the molecules.[40] The R_h measured by DLS and R_g ($\phi = 0$) were used to calculate P values for arborescent micelles in toluene-*d*. The P value for an ideal hard sphere is 0.775.[40] The P values for arborescent copolymer micelles in toluene-*d* were 0.65 ± 0.03 and 0.67 ± 0.03 for G1PS−P2VP5K and 30K, respectively, significantly smaller than 0.775. A P value below 0.775 suggests that the arborescent micelle corresponds to a sphere with a soft surface (transient outer shell) rather than an idealized hard sphere. The soft surface (transient shell) morphology of the arborescent micelles also implies that the P2VP shell of these molecules is unlikely to be fully collapsed into a dense shell in toluene-*d*. It was previously shown that in toluene the internal density of arborescent styrene homopolymers of the same generation as the copolymers used in the current investigation could be modeled as spheres with a transient outer region described by a power law model.[41] The power law function used was given by

$$\rho(r) - \rho_s = A\left(1 - \left(\frac{r}{R}\right)^\alpha\right) \qquad (6)$$

where R_{max} corresponds to the hydrodynamic radius and A is the contrast between the solvent and the center of the sphere. A single density profile with a power law function could be used to model the internal density of arborescent micelles, since the SLD of the PS and P2VP components is very similar and much smaller than the SLD of toluene-*d* ($\rho_{PS} = 1.4 \times 10^{-6}$ Å^{-2}, $\rho_{P2VP} = 1.77 \times 10^{-6}$ Å^{-2}, and $\rho_{toluene\text{-}d} = 5.66 \times 10^{-6}$ Å^{-2}). The fits to the SANS data using the power law model are

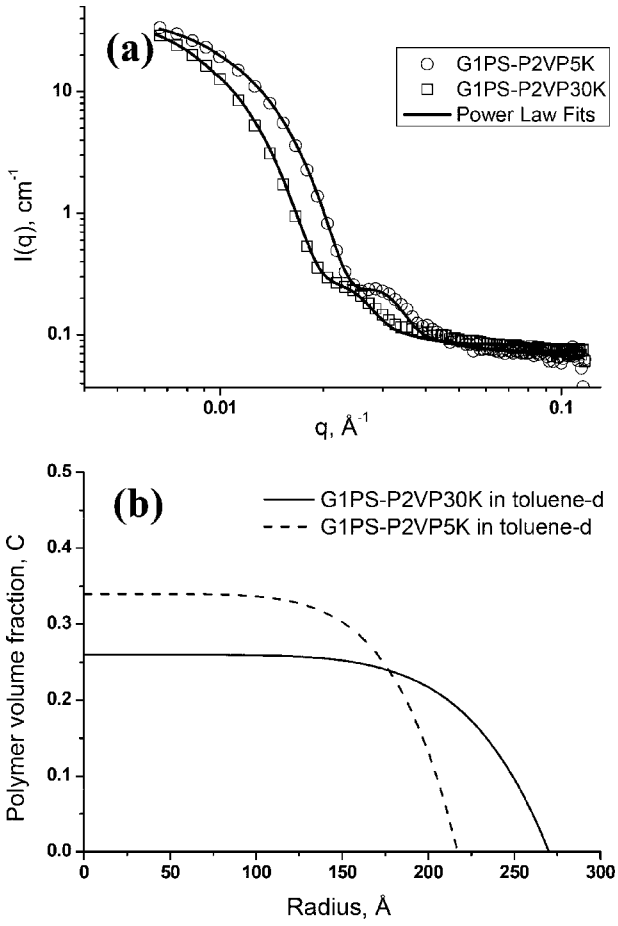

Figure 6. (a) SANS data for G1PS−P2VP5K ($\phi = 0.0034$ g/mL) and G1PS−P2VP30K ($\phi = 0.0034$ g/mL) in toluene-*d* at 75 °C and best fits using the power law model. The fit of the data includes about 10% polydispersity in size for the polymers and instrumental smearing effect. (b) Polymer fraction profiles for the copolymers in toluene-*d* derived from the power law model fits.

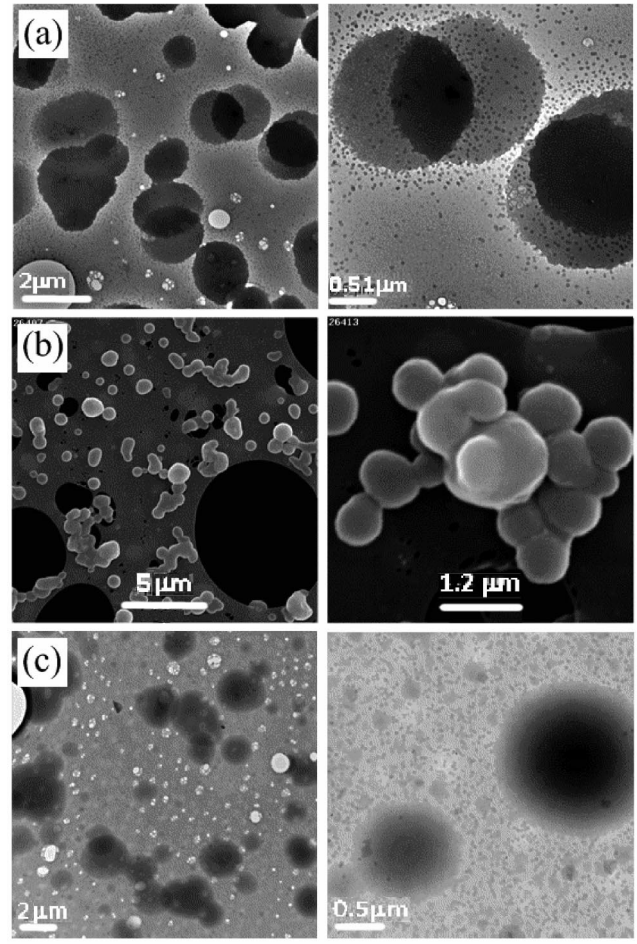

Figure 7. (a) TEM images for G1PS−P2VP5K, (b) SEM images for G1PS−P2VP5K, and (c) TEM images for G1PS−P2VP30K on holey carbon-coated grids after evaporation of the solutions in toluene ($\phi = 0.0014$ g/mL) at 20 °C.

provided in Figure 6a, and the corresponding polymer density profiles are displayed in Figure 6b. The $I(q)$ fits obtained using the core−shell model (Figure 3a) and the power law model (Figure 6a) are comparably good. However, the power law function gives larger overall dimensions for the unimolecular micelles than the core−shell model, closer to the R_h measured by DLS (Figure 1), suggesting that the model with a transient surface is a more realistic representation of the morphology of arborescent micelles in toluene-*d*. The α (exponent) value derived from the best fits was found to be $\alpha = 6$, larger than $\alpha = 4$ previously determined for arborescent styrene homopolymers in toluene-*d*.[35] The power law function with a larger α value leads to thinner (sharper) transient shell region, closer to the density profile of hard spheres. The larger $\alpha = 6$ of the arborescent PS−P2VP as compared to $\alpha = 4$ for arborescent PS in toluene-*d* is presumably due to the P2VP shell being less swollen than the shell of arborescent PS, since toluene-*d* is a good solvent for PS but a poor solvent for P2VP.

The aggregates were further investigated by TEM and SEM analysis. The images were recorded for samples prepared by the evaporation of dilute solutions ($\phi = 0.0014$ g/mL) on holey carbon-coated grids. For the SEM images, platinum was coated on the samples. The temperatures maintained during solvent evaporation were the same as the solution temperatures used in the DLS measurements. The aggregates of G1PS−P2VP5K obtained in toluene at 20 °C are depicted in Figure 7a,b. Large aggregates of relatively uniform size with a spherical shape are clearly seen in the TEM (Figure 7a) and SEM (Figure 7b) images, while pictures (not shown) recorded for the same solutions evaporated at 30 °C did not show such aggregates. The electron microscopy images in Figure 7 suggest that some of the large spheres tend to associate, which may occur during solvent evaporation. In Figure 7a, a higher resolution TEM image also shows the presence of smaller species, corresponding to the unimolecular micelles, at the periphery of the large aggregates. This indicates that some isolated molecules are present even below the critical self-assembly temperature. They were understandably not resolved in DLS analysis due to the dominant effect of the large spheres on the light scattering signal. The coexistence of isolated molecules and aggregates of arborescent copolymers, even below the cst, is very different from the formation of monodispersed (aggregated) micelles observed for conventional linear block and star copolymers below the cmt. TEM images recorded for the copolymers with long P2VP side chains (G1PS−P2VP30K) in toluene at 20 °C are provided in Figure 7c. The size and shape of the aggregates of copolymers with P2VP30K side chains were not significantly different from those observed for the shorter chain P2VP5K copolymers.

Conclusions

Amphiphilic arborescent copolymers incorporating a polystyrene (PS) core and a shell of poly(2-vinylpyridine) (P2VP) chains were investigated in toluene, a solvent selective for the PS core. The self-assembly behavior of the copolymers in toluene strongly depended on temperature. Above the cst, the

copolymers remained as unimolecular (nonassociated) micelles. SANS analysis indicated that the unimolecular micelles in toluene-*d* did not have a dense shell, in spite of the partial collapse of the P2VP segments. These unimolecular micelles self-assembled into supramolecular aggregates with a well-defined spherical topology at temperatures below the cst. The cst could be tuned to higher temperatures by increasing the length of the P2VP chains in the shell.

Acknowledgment. This research was supported by an appointment to the Postdoctoral Research Fellowship Program of the Australian Nuclear Science and Technology Organisation. The financial support of the Natural Sciences and Engineering Research Council of Canada is acknowledged for the synthetic part of the work. We acknowledge the support of the National Institute of Standards and Technology, U.S. Department of Commerce, in providing the neutron research facilities used in this work.

Supporting Information Available: Synthesis of arborescent copolymers, Guinier plots for SANS data, and concentration dependence of R_g. This material is available free of charge via the Internet at http://pubs.acs.org.

References and Notes

(1) Hamley, I. W. *Angew. Chem., Int. Ed.* **2003**, *42*, 1692–1712.
(2) Foster, S.; Plantenberg, T. *Angew. Chem., Int. Ed.* **2002**, *41*, 688–714.
(3) Hadjichristidis, N.; Pispas, S. *Adv. Polym. Sci.* **2006**, *200*, 37–55.
(4) Rodríguez-Hernández, J.; Chécot, F.; Gnanou, Y.; Lecommandoux, S. *Prog. Polym. Sci.* **2005**, *30*, 691–724.
(5) Tomalia, D. A. *Prog. Polym. Sci.* **2005**, *30*, 294–324.
(6) Smith, D. K.; Hirst, A. R.; Love, C. S.; Hardy, J. G.; Brignell, S. V.; Huang, B. *Prog. Polym. Sci.* **2005**, *30*, 220–293.
(7) Ornatska, M.; Peleshanko, S.; Genson, K. L.; Rybak, B.; Bergman, K. N.; Tsukruk, V. V. *J. Am. Chem. Soc.* **2004**, *126*, 9675–9684.
(8) Tomalia, D. A.; Brothers II, H. M.; Piehler, L. T.; Durst, H. D.; Swanson, D. R. *Proc. Natl. Acad. Sci. U.S.A.* **2002**, *99*, 5081–5087.
(9) Tomalia, D. A.; Swanson D. R. In *Dendrimers and Other Dendritic Polymers*; Fréchet, J. M. J., Tomalia, D. A., Eds.; Wiley: Chichester, 2001; pp 617−629.
(10) Tomalia, D. A. *Aldrichim.Acta* **2004**, *37*, 39–57.
(11) Taton, D.; Feng, X.; Gnanou, Y. *New J. Chem.* **2007**, *31*, 1097–1110.
(12) Voit, B. *J. Polym. Sci., Part A: Polym. Chem.* **2000**, *38*, 2505–2525.
(13) Teertstra, S. J.; Gauthier, M. *Prog. Polym. Sci.* **2004**, *29*, 277–327.
(14) Kee, R. A.; Gauthier, M. *Macromolecules* **2002**, *35*, 6526–6532.
(15) Gauthier, M.; Li, J.; Dockendorff, J. *Macromolecules* **2003**, *36*, 2642–2648.
(16) Knauss, D. M.; Al-Muallem, H. A.; Huang, T.; Wu, D. T. *Macromolecules* **2000**, *33*, 3557–3568.
(17) Hadjichristidis, N.; Iatrou, H.; Pitsikalis, M.; Mays, J. *Prog. Polym. Sci.* **2006**, *31*, 1068–1132.
(18) Hirao, A.; Tsunoda, Y.; Matsuo, A.; Sugiyama, K.; Watanabe, T. *Macromol. Res.* **2006**, *14*, 272–286.
(19) Hutchings, L. R.; Roberts-Bleming, S. J. *Macromolecules* **2006**, *39*, 2144–2152.
(20) Hutchings, L. R.; Dodds, J. M.; Roberts-Bleming, S. J. *Macromolecules* **2005**, *38*, 5970–5980.
(21) Erdodi, G.; Ivan, B. *Chem. Mater.* **2004**, *16*, 959–962.
(22) Malynych, S.; Luzinov, I.; Chumanov, G. *J. Phys. Chem. B* **2002**, *106*, 1280–1285.
(23) Ionov, L.; Sapra, S.; Synytska, A.; Rogach, A. L.; Stamm, M.; Diez, S. *Adv. Mater.* **2006**, *18*, 1453–1457.
(24) Tokareva, I.; Minko, S.; Fendler, J. H.; Hutter, E. *J. Am. Chem. Soc.* **2004**, *126*, 15950–15951.
(25) Sikora, A.; Tuzar, Z. *Makromol. Chem.* **1983**, *184*, 2049–2059.
(26) Oostergetel, G. T.; Esselink, F. J.; Hadziioannou, G. *Langmuir* **1995**, *11*, 3721–3724.
(27) Voulgaris, D.; Tsitsilianis, C.; Esselink, F. J.; Hadziioannou, G. *Polymer* **1998**, *39*, 6429–6439.
(28) Voulgaris, D.; Tsitsilianis, C.; Grayer, V.; Esselink, F. J.; Hadziioannou, G. *Polymer* **1999**, *40*, 5879–5889.
(29) Gorodyska, G.; Kiriy, A.; Minko, S.; Tsitsilianis, C.; Stamm, M. *Nano Lett.* **2003**, *3*, 365–368.
(30) Krishnamoorthy, S.; Pugin, R.; Brugger, J.; Heinzelmann, H.; Hoogerwerf, A. C.; Hinderling, C. *Langmuir* **2006**, *22*, 3450–3452.
(31) Yun, S. I.; Briber, R. M.; Kee, R. A.; Gauthier, M. *Polymer* **2006**, *47*, 2750–2759.
(32) Glinka, C. J.; Barker, J. G.; Hammouda, B.; Krueger, S.; Moyer, J. J.; Orts, W. J. *J. Appl. Crystallogr.* **1998**, *31*, 430–445.
(33) Yun, S. I.; Briber, R. M.; Kee, R. A.; Gauthier, M. *Polymer* **2003**, *44*, 6579–6587.
(34) Connolly, R.; Timoshenko, E. G.; Kuznetsov, Y. A. *Macromolecules* **2004**, *37*, 7381–7392.
(35) Giupponi, G.; Buzza, D. M. A. *J. Chem. Phys.* **2005**, *122*, 194903.
(36) Hayter, J. B. In *Physics of Amphiphiles: Micelles, Vesicles and Microemulsions*; Degiorgio, V., Corti, M., Eds.; North Holland: Amsterdam, 1983; pp 59−93.
(37) Glatter, O. *J. Appl. Crystallogr.* **1979**, *12*, 166–175.
(38) Yun, S. I.; Lai, K. C.; Briber, R. M.; Teertstra, S. J.; Gauthier, M.; Bauer, B. J. *Macromolecules* **2008**, *41*, 175–183.
(39) Svergun, D. I.; Koch, M. H. J. *Rep. Prog. Phys.* **2003**, *66*, 1735–1782.
(40) Antonietti, M.; Bremser, W.; Schmidt, M. *Macromolecules* **1990**, *23*, 3796–3805.
(41) Choi, S.; Briber, R. M.; Bauer, B. J.; Topp, A.; Gauthier, M.; Tichagwa, L. *Macromolecules* **1999**, *32*, 7879–7886.

MA801222V